Ginsenoside Rg1 Accelerates Paracrine Activity and Adipogenic Differentiation of Human Breast Adipose-Derived Stem Cells in a Dose-Dependent Manner *In Vitro*

Zhi-Jie Liang[1,2], Xiang Lu[3], Dan-Dan Zhu[4], Xiao-Lin Yi[4],
Fang-Xiao Wu[4], Ning He[4], Chao Tang[5], Chang-Yuan Wei[1] [ID],
and Hong-Mian Li[4]

Abstract

Augmenting the biological function of adipose-derived stromal cells (ASCs) is a promising approach to promoting tissue remodeling in regenerative medicine. Here, we examined the effect of ginsenoside Rg1 on the paracrine activity and adipogenic differentiation capacity of human breast ASCs (hbASCs) *in vitro*. hbASCs were isolated and characterized in terms of stromal cell surface markers and multipotency. Third-passage hbASCs were cultured in basic media only or basic media containing different concentrations of G-Rg1 (0.1–100 μM). Cell proliferation was assessed by CCK-8 assay. Paracrine activity was assessed using ELISA. Gene expression was measured by qRT-PCR. Adipogenic differentiation capacity was evaluated by Oil red O staining. We found that hbASCs differentiated into adipocytes, osteoblasts, and chondrocytes in appropriate induction culture medium. hbASCs showed expression of CD29, CD44, CD49d, CD73, CD90, CD105, and CD133 but not CD31 and CD45 surface markers. G-Rg1 increased hbASC proliferation and adipogenic differentiation capacity at lower concentrations (0.1–1 μM) and had the opposite effects at higher concentrations (10–100 μM), while enhanced paracrine activity was observed in all experimental groups compared with control group, and the activation effect of lower concentration G-Rg1 was greater than at higher concentration. These results indicate that G-Rg1 can enhance the proliferation, paracrine activity, and adipogenic differentiation capacity of hbASCs within a certain concentration range. Therefore, the use of G-Rg1 may be beneficial to ASC-assisted fat graft regeneration and soft tissue engineering.

Keywords

human breast adipose-derived stem cells, ginsenoside Rg1, paracrine, proliferation, adipogenic differentiation, gene expression

[1] Department of Breast Surgery, The Affiliated Tumor Hospital of Guangxi Medical University, Nanning, China
[2] Department of Breast and Thyroid Surgery, The Fifth Affiliated Hospital of Guangxi Medical University &The First People's Hospital of Nanning, Nanning, China
[3] Department of Hematology, The Fifth Affiliated Hospital of Guangxi Medical University & The First People's Hospital of Nanning, Nanning, China
[4] Department of Plastic and Aesthetic Surgery, The Fifth Affiliated Hospital of Guangxi Medical University & The First People's Hospital of Nanning, Nanning, China
[5] Department of Plastic and Aesthetic Surgery, The Mengxiang Plastic Hospital, Nanning, China

Corresponding Authors:
Chang-Yuan Wei, Department of Breast Surgery, The Affiliated Tumor Hospital of Guangxi Medical University, Nanning, 530021, China.
Email: weichangyuan@gxmu.edu.cn

Hong-Mian Li, Department of Plastic and Aesthetic Surgery, The Fifth Affiliated Hospital of Guangxi Medical University & The First People's Hospital of Nanning, Nanning 530022, China.
Email: lihongmian@gxmu.edu.cn

Introduction

Irreversible soft tissue loss caused by congenital defects, degeneration, trauma, or tumor resection is generally associated with physical, physiological, and psychological problems. Fat grafting is widely accepted as a preferred treatment for tissue volume reconstruction. However, the unpredictable absorption rates of adipose tissue, ranging from 20% to 90%, greatly influence the retention of fat grafts due to fat resorption, fibrosis, and calcification, which limits their therapeutic efficacy[1,2]. To address this issue, a novel strategy called cell-assisted lipotransfer was developed, in which the fat tissue transplant is combined with a stromal vascular fraction containing abundant adipose-derived stromal cells (ASCs). In the early stage after autologous free fat transplantation, nutrient diffusion and neovascularization are urgently required for avascular fat graft survival. ASCs, which can differentiate into endothelial cells[3,4], promote the mobilization and recruitment of endothelial cells by secreting proangiogenic and antiapoptotic factors, such as vascular endothelial growth factor (VEGF) and basic fibroblast growth factor (bFGF), which play critical roles in accelerating angiogenesis[5–7]. Furthermore, several cytokines secreted by ASCs participate in immune responses and the reconstruction and remodeling of graft tissue[8–10]. In addition to retention of the fat graft, skin rejuvenation, and lesion healing are frequently observed around the recipient site, and are considered beneficial outcomes of the paracrine activity of ASCs. Several studies show that surviving fat grafts after cell-assisted lipotransfer consist of a mixture containing ASC-differentiated adipocytes and mature adipocytes[11], suggesting that adipogenic differentiation allows ASCs to serve as cellular resources for adipose tissue reconstruction, and that adipogenic differentiation-optimized methods could promote adipose implant enlargement[12,13]. Although ASC-assisted transplantation shows promise for tissue regeneration, its efficacy varies due to the inconsistent function of ASCs.

Ginsenoside Rg1(G-Rg1), a steroidal saponin isolated from ginseng, protects against cerebral and myocardial infarction in animal models[14–17]. In addition, G-Rg1 promotes angiogenesis by inducing biological activity of human umbilical vein endothelial cells and endothelial progenitor cells[18–21], promotes ASC growth and differentiation into a neural phenotype *in vitro*[22,23], and increases microvessel density and adipogenesis in transplants *in vivo* by enhancing relative gene expression[24]. For pharmacologic application, G-Rg1 could optimize the functional benefits of ASCs in combination with lipofilling in a dose-dependent manner. We previously found that the proliferation and neural differentiation of ASCs responds dose-dependently to G-Rg1 *in vitro*, consistent with research using mouse-derived ASCs[22,23]. Moreover, we found that the chondrogenic differentiation of human breast ASCs (hbASCs) depended on G-Rg1 concentration[25]. Thus, G-Rg1 may be a candidate adjuvant for ASC application in tissue remodeling, although how G-Rg1 influences the biological function of ASCs is not yet well understood. Therefore, we examined the effects of G-Rg1 on the paracrine activity and adipogenic differentiation capacity of hbASCs.

Materials and Methods

Patient Consent and Ethical Approval

The present study was approved by the institutional ethical review board of Guangxi Medical University (Nanning, Guangxi, China). Written informed consent was provided by the donor patient.

Isolation and Identification of hbASCs

hbASCs were isolated and cultured as previously described[24,25] from spare breast adipose tissue from a 23-year-old healthy female patient without history of breast-feeding, who underwent breast reduction surgery, with body mass index (BMI) = 26.57 kg/m2 (height: 1.68 m, weight: 75 kg). P1 and P3 cells were analyzed using a Becton Dickinson FACSm Calibur flow cytometer. Cells (1 mL, 1×10^6/mL) were incubated with fluorescein isothiocyanate (FITC)- or phycoerythrin (PE)-conjugated antibodies for 30 min. The following surface markers were used: CD29/PE, CD34/FITC, CD44/PE, CD45/FITC, CD49d/PE, CD73/PE, CD90/PE, CD105/PE, and CD133/FITC (BD Biosciences, Franklin Lakes, NJ, USA). Incubation with negative control IgG-PE antibodies was performed in the dark at room temperature for 30 min. Cell Quest Pro acquisition software (BD Biosciences) was used for data analysis. To assess cell differentiation, P3 hbASCs were cultured in adipogenic (DMEM, 10% FBS, 1% antibiotic/antimycotic, 200 µM indomethacin, 0.5 mM isobutyl-methylxanthine, 1 µM dexamethasone, 10 µM insulin), osteogenic (DMEM, 10% FBS, 1% antibiotic/antimycotic, 0.1 M dexamethasone, 50 µM ascorbate-2-phosphate, 10 mM b-glycerophosphate), or chondrogenic (DMEM, 1% FBS, 10 ng/ml TGF-β1, 1% antibiotic/antimycotic, 6.25 µg/ml insulin, 50 nM ascorbate-2-phosphate) culture media for 2–3 weeks, after which the relative staining method was performed.

For assessing adipogenic or osteogenic differentiation, differentiation medium were removed from the wells after 2–3 weeks induced culture, the cells were then rinsed with PBS, and fixed with 2 mL of 4% formaldehyde solution for 30 min; 1 ml oil red O working solution or 1 ml alizarin red S were added into one well to stain the cells for 3–5 min after being washed twice with PBS, and the cells then could be visualized and analyzed by microscope.

For assessing chondrogenic differentiation, the pellet was fixed with formalin, embedded with paraffin, sliced into 3–4 µm paraffin sections, and stained with the alcian blue solution for 30 min. The cells were washed in running tap water for 2 min, and visualized and analyzed by microscope.

Table 1. qPCR Primer Sequences for Paracrine- and Adipogenesis-Related Target Genes.

Gene	Forward	Reverse
HIF-1α	GAAGAACTTTTAGGCCGCTCA	AGTCGTGCTGAATAATACCAC
miRNA-31	AGGCAAGATGCTGGCATAGC	CAGTGCAGGGTCCGAGGTAT
FIH-1	ATAGGCGGAGCTTCCGGTTC	GAATGGGCCTAGTCGGGAAG
VEGF	CTTGCCTTGCTGCTCTACCTCC	CACACTCCAGGCCCTCGTCA
FGF-2	GCGACCCTCACATCAAGCTAC	CCAGTTCGTTTCAGTGCCACA
EGF	GACTGTGCTCCTGTGGGATG	GGTGGAGTAGAGTCAAGACAGTGA
PDGF	CCACTAAGCATGTGCCCGAGA	TGGCACTTGACACTGCTCGT
ANG	CCCTGCAAAGACATCAACACA	AGGTAAGCCATTTTCACAAGCA
TGF-β1	TACCTGAACCCGTGTTGCTCT	CTGCCGCACAACTCCGGTGA
IL-10	AGCTGTGGCCAGCTTGTTAT	TTCCATCTCCTGGGTTCAAG
CXCR4	CAATGACTTGTGGGTGGTTG	GAAAGCCAGGATGAGGATG
TIMP-1	CCTTATACCAGCGTTATGAGATCAA	AGTGATGTGCAAGAGTCCATCC
PPARγ2	TGTCTCATAATGCCATCAGGT	TCTTTCCTGTCAAGATCGC
FAD24	GGGAACTTGAGGAAGAGATCATTG	GGATCTGATAATATGGCAGATGCC
C/EBPα	GCCGCGCACCCCGACCTCC	CCCCGCAGCGTGTCCAGTTCG
ADD1	AGTACAAAGCCAAGTCCCGTTC	CCCGAATCACCGTCACTAGCAA
GAPDH	CAAATTCCATGGCACCGTCA	GACTCCACGACGTACTCAGC

Cell Proliferation

The proliferation of third-passage hbASCs was examined using the CCK-8 method. Cells were transferred to a 96-well plate at a density of 2×10^4 cells/well and cultured for 24 h in an incubator at 37°C with 50 mL/L CO_2, after which the normal nutrient solution was poured off. Cells were then randomly divided into five groups with six wells/group: basic media (BM) only without fetal bovine serum and antibiotics (control), BM + 0.1 μM G-Rg1, BM + 1 μM G-Rg1, BM + 10 μM G-Rg1, and BM + 100 μM G-Rg1. After an additional 10 days of culture, during which liquid supernatant was removed daily at the same time for each group, 50 μL CCK-8 working fluid was added to each well followed by 4 h of culture. After 10-min oscillations, optical density at 450 nm was detected using a microplate reader to generate proliferation curves.

Paracrine Activity

Five groups of hbASCs were cultured in 12-well plates at a density of 2×10^4 cells/well with different concentrations of G-Rg1 (0–100 μM) in an incubator at 37°C with 50 mL/L CO_2 for 14 days. After 7 and 14 days, supernatants were collected for analysis by enzyme-linked immunosorbent assay (ELISA). Levels of VEGF, FGF-2, epidermal growth factor (EGF), insulin-like growth factor (IGF)-1, stromal cell-derived factor (SDF)-1, platelet-derived growth factor (PDGF), angiopoietin (ANG), transforming growth factor-beta 1 (TGF-β1), tissue inhibitor of metalloproteinase (TIMP)-1, and interleukin (IL)-10 were measured using Quantikine colorimetric ELISA kits (R&D Systems, Minneapolis, MN, USA) according to the manufacturer's instructions.

Adipogenic Differentiation Capacity

hbASCs treated with different concentrations of G-Rg1 (0–100 μM) were cultured under an adipogenic induction condition for 2 weeks and then stained with Oil Red O. Adipocyte densities were measured in a double-blind manner in five visual fields under the same magnification. Cell numbers were normalized to square millimeters. Lipids were extracted from cells with 100% isopropanol and gentle shaking for 5 min. Lipid concentrations were measured based on absorbance at 510 nm in triplicate for each sample.

Quantitative reverse transcription polymerase chain reaction. Total RNA was extracted using Trizol reagent (Invitrogen, Carlsbad, CA, USA) and treated with DNase I. cDNA conversion was performed using a RevertAid™ First Strand Synthesis Kit (Fermentas, Waltham, MA, USA). Quantitative reverse transcription polymerase chain reaction (qRT-PCR) was performed using SYBR® Green PCR Master Mixes on a StepOne-Plus Real-Time PCR System (Applied Biosystems, Foster City, CA, USA) with primer pairs for paracrine- and adipogenesis-related factors (Table 1). Relative gene expression was analyzed using the $2^{-\Delta\Delta Ct}$ method and normalized to GAPDH expression. Data are presented as fold change relative to control.

Statistical Analysis

Data are shown as mean $\pm$ standard deviation (SD). Analysis of variance (ANOVA) was performed to test for differences among groups, thereby accounting for intra- and inter-group variation. Following significant ANOVAs, multiple pairwise comparisons were performed using paired t-tests. Statistical significance was set at two-tailed $P < 0.05$. Data were analyzed using SPSS for Windows version 17.0 (Chicago, IL, USA).

Results

Morphological Characterization and Multipotentiality of hbASCs

hbASCs began to adhere 6 h after seeding. Cells were initially small, round, and of non-uniform size with some

mononuclear blood cells. They gradually stretched into short or long spindle shapes by 48 h, and showed typical fibroblast-like morphology after the third passage. Primary hbASCs reached 80–90% confluence after 7–8 days (Fig. 1A I), whereas P1 hbASCs reached the same confluence in 3–4 days with a 1:3 split ratio (Fig. 1A II-III). P3 hbASCs were cultured under adipogenic, osteogenic, and chondrogenic induction conditions, and lineage-specific morphologies of hbASCs were observed after 2 weeks, 3 weeks, and 2 weeks, respectively. Adipogenic, osteogenic, and chondrogenic differentiation were identified by positive Oil Red O (Fig. 1A IV-V), Alizarin red (Fig. 1A VI-VII), and Alcian blue (Fig. 1A VIII-IX) staining, respectively, validating the multipotency of hbASCs.

Immunophenotypic Characterization of hbASCs

P1 hbASCs expressed the mesenchymal surface markers CD29 (Fig. 1A I), CD44 (Fig. 1A III), CD49d (Fig. 1B V), CD73 (Fig. 1B VI), CD90 (Fig. 1B VII), CD105 (Fig. 1B VIII), and CD166 (Fig. 21B IX), but not CD34 (Fig. 1B II) or CD45 (Fig. 1B IV) as determined by flow cytometry analysis (Fig. 1C).

hbASC Proliferation

hbASCs were cultured in BM containing 0, 0.1, 1, 10, or 100 μM G-Rg1, and CCK-8 tests were performed at 1–10 days. Compared with the control group (BM), cells in the 0.1 and 1 μM G-Rg1 groups had higher OD values, whereas cells in the 10 and 100 μM G-Rg1 groups had lower OD values at all time points after day 3 (Fig. 2A). Cell proliferation reached a plateau on day 6 for all groups. These growth curves show that G-Rg1 affected hbASC proliferation in a dose-dependent manner, with cell proliferation declining in culture media containing ≥ 10 μM G-Rg1.

Paracrine Activity of hbASCs

After culture for 7 and 14 days, concentrations of VEGF, FGF-2, EGF, SDF-1, PDGF, ANG, TGF-β1, TIMP-1, and IL-10 in the supernatant were measured by Quantikine colorimetric sandwich ELISA. Compared with the control group (BM), cytokine concentrations were higher in the 0.1 and 1 μM G-Rg1 groups and lower in the 10 and 100 μM G-Rg1 groups at both time points (Fig. 2B), suggesting that G-Rg1 promotes the paracrine activity of hbASCs in dose-dependent manner within a low concentration range.

Paracrine- and Angiogenesis-Related Gene Expression in hbASCs

qRT-PCR on day 7 showed that gene expression of the paracrine-related factors VEGF, FGF-2, EGF, SDF-1, PDGF, ANG, TGF-β1, TIMP-1, and IL-10 was higher in the 0.1 and 1 μM G-Rg1 groups and lower in the 10 and 100 μM G-Rg1 groups compared with the control (BM) group (Fig. 2C). Gene expression of the angiogenesis-related factors HIF-1α and CXCR4 as well as miRNA31 varied in a similar dose-dependent manner. By contrast, gene expression of FIH-1 was lower in the 0.1 and 1 μM G-Rg1 groups and higher in the 10 and 100 μM G-Rg1 groups.

Adipogenic Differentiation of hbASCs

Oil Red O staining was used to assess adipogenic differentiation capacity 14 days after adipogenic induction. Compared with the control (BM) group, more stained cells were observed in the 0.1 and 1 μM G-Rg1 groups, and fewer stained cells were observed in the 10 and 100 μM G-Rg1 groups (Fig. 3A). Quantification data showed a ～50% increase in stained cells in the 0.1 and 1 μM G-Rg1 groups and a ～50% decrease in stained cells in the 10 and 100 μM G-Rg1 groups (Fig. 3B,C).

Adipogenic Marker Gene Expression in hbASCs

At 14 days after adipogenic induction, gene expression of peroxisome proliferator-activated receptor-γ (PPARγ), factor for adipocyte differentiation 24 (FAD24), CCAAT/enhancer binding protein-α (C/EBPα), and adducin 1 (ADD1) was higher in the 0.1 and 1 μM G-Rg1 groups and lower in the 10 and 100 μM G-Rg1 groups compared with the control (BM) group (Fig. 3D).

Discussion

Although the efficacy of ASC-assisted lipofilling has been repeatedly confirmed in recent decades[26–28], controversies over the survival and regeneration mode of fat graft tissue still exist. Previous studies provide insight into the histological changes in fat transplants, revealing that transplanted adipose grafts can be divided into three regions: (1) an innermost area where both adipocytes and ASCs die; (2) a periphery zone where adipocytes and ASCs survive; and (3) an intermediate area where adipocytes die but ASCs survive and regenerate, which is considered to contribute to fat graft remodeling and retention[11]. The proliferation and adipogenic differentiation of ASCs are commonly believed to play important roles in fat graft enlargement. Kølle et al. report that higher numbers of ASCs in a lipograft positively affects the final graft take, evidenced by a nearly 5-fold greater adipose tissue retention of ASC-enriched fat grafts compared with a control condition, as well as observations of more mature adipocytes and less necrotic fibrosis[29]. Beside the ASCs, more and more scientists found there are other cells in fat tissue, called dedifferentiated fat (DFAT) cells, which are considered as the other "seed cell" resource for regenerative medicine since they possess multidirectional differentiation capacity similar to ASCs[30], suggesting differentiating into mature cell plays critical role in tissue regeneration. From this perspective, several techniques have
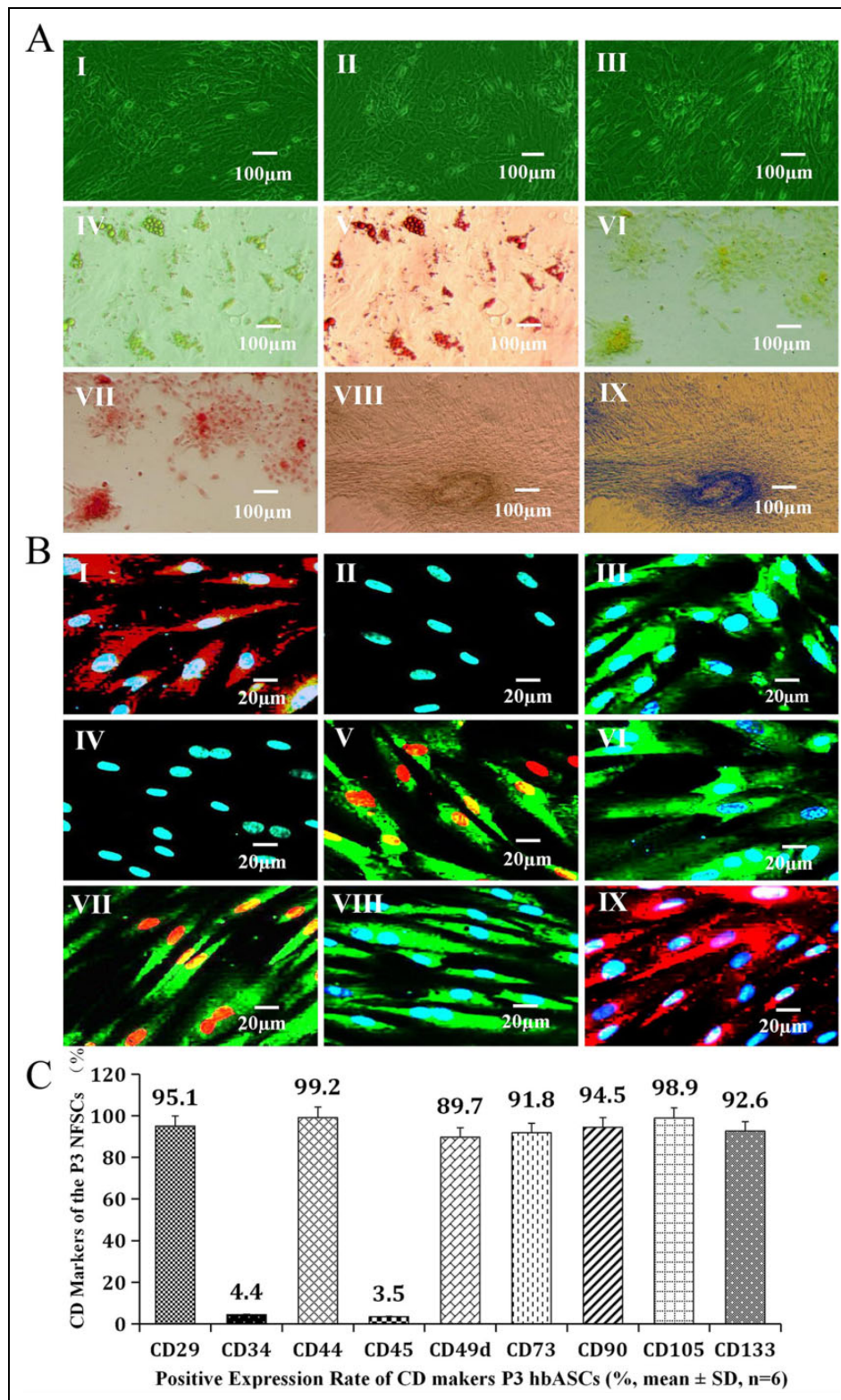
Fig. 1. (A) Characterization of hbASCs. (I) Initial isolation and culture of primary hbASCs for 7–8 days. (II) P1 hbASCs cultured for 3–4 days with a 1:3 split ratio. (III) P3 hbASCs cultured for 3–4 days with a 1:3 split ratio. (IV) Adipogenic induction for 2 weeks. (V) Positive Oil Red O staining after adipogenic induction. (VI) Osteogenic induction for 3 weeks. (VII) Alizarin red staining after osteogenic induction. (VIII) Chondrogenic induction for 2 weeks. (IX) Alcian blue staining after chondrogenic induction. (B) Immunophenotypic characterization of hbASCs. The mesenchymal surface markers (I) CD29, (II) CD44. (V) CD49d, (VI) CD73, (VII) CD90, (VIII) CD105, and (IX) CD166, but not (II) CD34 or (IV) CD45 were expressed in all P1 hbASCs as determined by flow cytometry. (C) Immunofluorescence staining of P3 hbASCs demonstrated expression of CD29, CD44, CD49d, CD73, CD90, CD105, and CD133, but not CD34 or CD45 ($n = 6$).
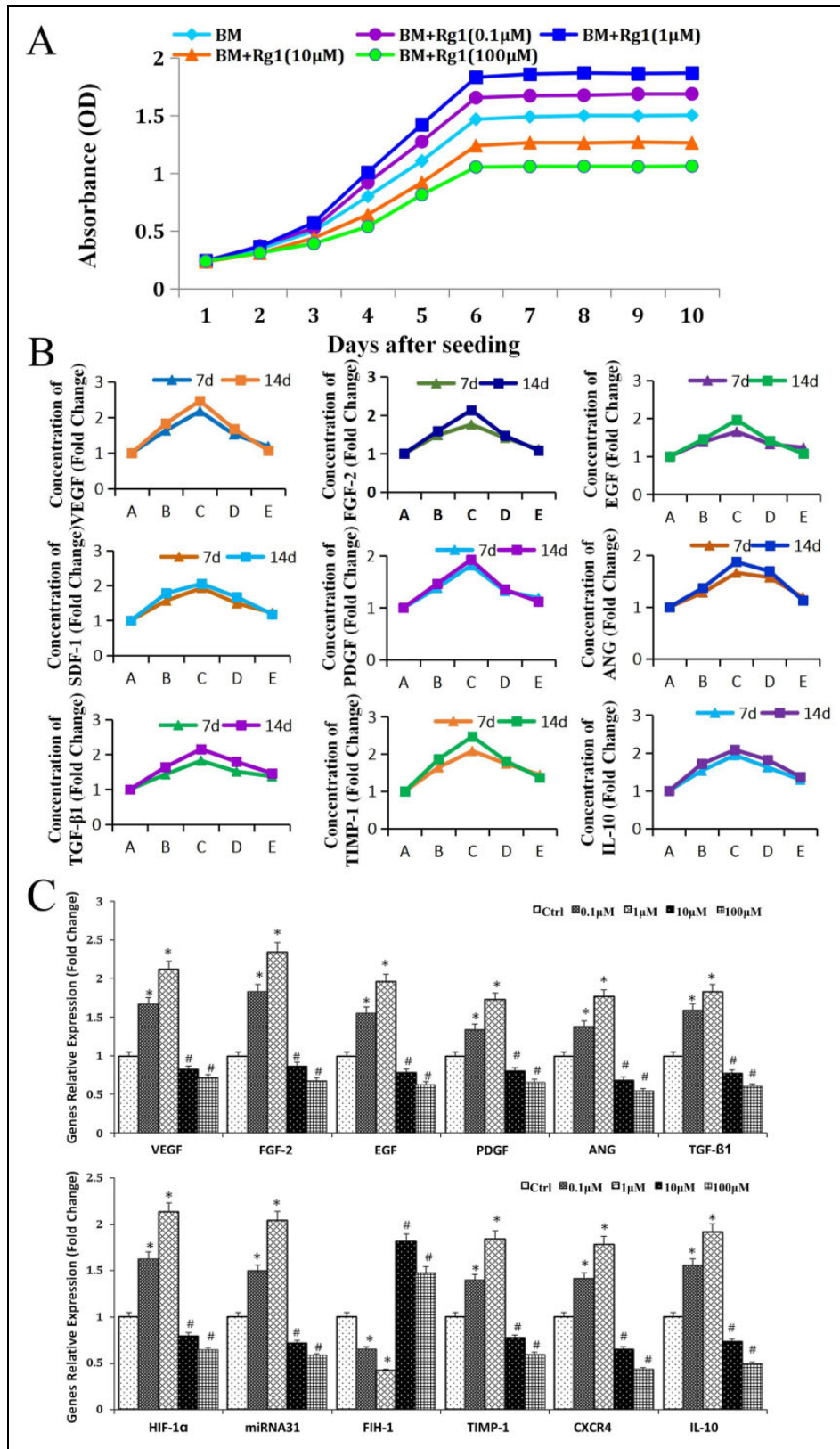
Fig. 2. (A) CCK-8 testing of hbASCs after 1–10 days of culture in BM only or BM containing 0, 0.1, 1, 10, or 100 μM G-Rg1. Data are presented as means. (B) Concentrations of VEGF, FGF-2, EGF, SDF-1, PDGF, ANG, TGF-β1, TIMP-1, and IL-10 in the supernatant of hbASCs cultured in BM only or BM containing 0.1, 1, 10, or 100 μM G-Rg1 after 7 and 14 days. (C) Relative mRNA expression of VEGF, FGF-2, EGF, PDGF, ANG, TGF-β1, HIF-1, miRNA31, FIH-1, TIMP-1, CXCR4, and IL-10 in hbASCs cultured in BM only or BM containing 0.1, 1, 10, or 100 μM G-Rg1 after 7 days. *$P < 0.05$ vs. BM; #$P < 0.05$ vs. BM.
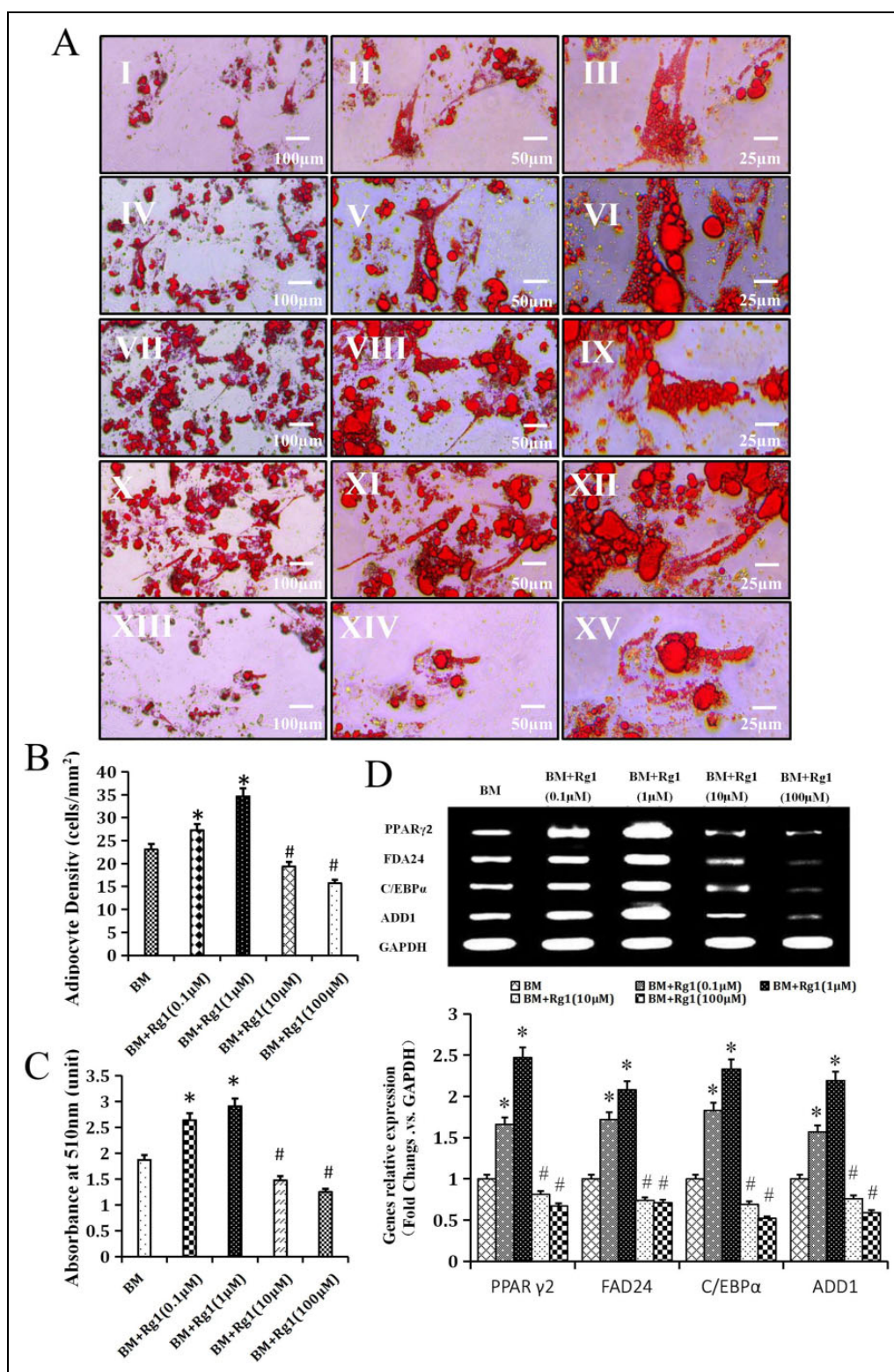
Fig. 3. (A) Adipocyte morphology and quantity were detected in five visual fields under the same magnification 14 days after adipogenic induction. Compared with the BM group (I–III), more oil red O-stained cells were observed in the 0.1 μM (IV–VI) and 1 μM (VII–IX) G-Rg1 groups, and fewer stained cells were observed in the 10 μM (X–XII) and 100 μM (XIII–XV) G-Rg1 groups (I, IV, VII, X, XII: ×100, II, V, VIII, XI, IV: ×200, III, VI, IX, XII, XV: ×400 magnification). (B), (C) Quantitative measurement of adipogenesis differentiation capacity. Compared with the BM group, adipocyte density (upper) and intracellular lipid content (lower) were increased in the 0.1 and 1 μM G-Rg1 groups and decreased in the 10 and 100 μM G-Rg1 groups (*$P < 0.05$ vs. BM, **$P < 0.05$ vs. BM). (D) Expression of PPARγ, FAD24, C/EBPα, and ADD1 in the BM only group and the 0.1, 1, 10, and 100 μM G-Rg1 groups (*$P < 0.05$ .vs. BM, #$P < 0.05$ vs. BM).

been developed to optimize the efficacy of ASCs in fat transplantation, such as drug stimulation, physical treatment, or gene modification[7,13,31,32]. By contrast, Yuan et al. report that most transplanted ASCs die during the 1st week after transplantation and suggest that angiogenic growth factors (e.g., VEGF, EGF) secreted by ASCs increase the neovascularization density of fat grafts[33]. Besides the secretion of paracrine factors, our recent findings indicate that a portion of retained hbASCs in fat grafts differentiate into vascular endothelial cells, becoming an extra cell source for new vessel formation, and that CXCR4-modified ASCs enhance the neovascularization density of fat grafts[34]. Neovascularization in the early stage after transplantation is critical to long-term fat retention and is associated with an increased number of inflammatory cells[33]. This phenomenon suggests that immune activity contributes to angiogenesis, consistent with the theory of tumor angiogenesis, and that immunologic factors secreted by ASCs (e.g., TGF-β1[35], IL-10) are responsible for the enhanced density of neovascularization in fat grafts[36]. We previously observed adipogenic differentiation and increased paracrine activity of ASCs in adipose grafts, suggesting both above-mentioned regeneration modes play important roles in ASC-assisted fat grafting, and that graft take is enhanced when ASCs are pretreated with certain drugs or genetic modifications[22,33]. We suspect that the variable efficacy of ASCs in fat grafting results from different optimization methods between studies, which may induce different fat graft regeneration modes. Several modifications of the biological function of ASCs have been developed to improve the survival of fat grafts[37–39], some of which have been found efficacious in clinical practice[40], suggesting ASC optimization as a potential research direction in the field of regenerative medicine.

G-Rg1 is the active component in ginseng, which has repeatedly been shown to optimize the biological function of ASCs[22,24,25], but the mechanism of this effect has not been well understood. In the present study, we found that G-Rg1 improved the paracrine activity of ASCs in a dose-dependent manner. More specifically, the levels of paracrine factors including angiogenic factors (VEGF, FGF-2, EGF, PDGF, and ANG), immunologic factors (SDF-1, TGF-β1, and IL-10), and the matrix remodeling factor TIMP-1 were higher in all experimental groups compared with control group, while the paracrine factors' concentration increased more greater in media containing lower G-Rg1 concentrations (0–1 μM) than higher G-Rg1 concentrations (10–100 μM). Also, lower concentrations of G-Rg1 were associated with increased expression of genes associated with paracrine factors, angiogenesis, and adipogenic differentiation as well as increased proliferation and adipogenic differentiation capacity of hbASCs, whereas these biological functions of ASCs were inhibited by concentrations of G-Rg1 $\geq$ 10 μM. These results support our recent finding that the tissue regeneration capacity of ASCs is improved after treatment with 10 μg/mL G-Rg1[39], suggesting G-Rg1 as a candidate promoter of ASC-assisted fat engraftment through its effects on the growth, differentiation, and paracrine activity of ASCs.

To the best of our knowledge, the dose-response relationship between G-Rg1 and ASC-assisted fat graft retention *in vivo* has not yet been described in detail. Our results suggest that the regulatory effects of G-Rg1 on cell proliferation and adipogenic differentiation at lower concentrations are opposite to those at higher concentration. In the meantime, the results revealed that the paracrine activity of hbASCs was enhanced by G-Rg1 at all concentration levels, but more significantly in lower concentrations than at higher concentrations, while the gene expression of those paracrine factors as inhibited at concentrations of G-Rg1 $\geq$ 10 μM. So we considered that paracrine activation may be more sensitive to G-Rg1, although the specific mechanism remains to be explored in our future research. All in all, the study indicated that the concentration of G-Rg1 may influence the efficacy of hbASCs in adipose tissue regeneration. To optimize the application of G-Rg1 in ASC-assisted tissue reconstruction, the mechanisms underlying the effects of G-Rg1 on ASC adipogenic differentiation and paracrine activity must be addressed in future *in vivo* experiments.

In conclusion, our results indicate that G-Rg1 can positively influence the proliferation, paracrine activity, and adipogenic phenotype differentiation of hbASCs *in vitro*. More specifically, lower and higher concentrations of G-Rg1 may have opposing effects on the biological function of hbASCs, suggesting that the optimum concentration of G-Rg1 should be determined in future experiments.

Authors' Note

Zhi-Jie Liang and Xiang Lu contributed equally to this work.

Author Contributions

Conceptualization, CW and HL; Formal analysis, DZ and XY; Investigation, ZL, XL and FW; Project administration, CW; Resources, CT; Software, FW; Supervision, HL; Writing original draft, ZL, DZ, XY and NH; Review & editing, XL, CW and HL.

Ethical Approval

All of the human ASC experiments were performed with the approval of Guangxi Medical University.

Statement of Human and Animal Rights

The present study was approved by the institutional ethical review board of Guangxi Medical University (Nanning, Guangxi, China). Written informed consent was provided by the donor patient.

Statement of Informed Consent

Informed consent was obtained from the human subjects used in this article.

Declaration of Conflicting Interests

The author(s) declared no potential conflicts of interest with respect to the research, authorship, and/or publication of this article.

ORCID iD

Chang-Yuan Wei   https://orcid.org/0000-0001-9776-2738

References

1. Illouz YG. Present results of fat injection. Aesthetic Plast Surg. 1988;12(3):175–181.

2. Ersek RA. Transplantation of purified autologous fat: a 3-year follow-up is disappointing. Plast Reconstr Surg. 1991;87(2):219–227; discussion 228.

3. Shi Z, Neoh KG, Kang ET, Poh CK, Wang W. Enhanced endothelial differentiation of adipose-derived stem cells by substrate. J Tissue Eng Regen Med. 2014;8(1):50–58.

4. Ning H, Liu G, Lin G, Yang R., Lue TF, Lin CS. Fibroblast growth factor 2 promotes endothelial differentiation of adipose tissue-derived stem cells. J Sex Med. 2009;6:967–979.

5. Ratushnyy A, Ezdakova M, Yakubets D, Buravkova L. Angiogenic activity of human adipose-derived mesenchymal stem cells under simulated microgravity. Stem Cells Dev. 2018;27(12):831–837.

6. Horikoshi-Ishihara H, Tobita M, Tajima S, Tanaka R, Oshita T, Tabata Y, Mizuno H. Coadministration of adipose-derived stem cells and control-released basic fibroblast growth factor facilitates angiogenesis in a murine ischemic hind limb model. J Vasc Surg. 2016;64(6):1825–1834.e1.

7. Khan S, Villalobos MA, Choron RL, Chang S, Brown SA, Carpenter JP, Tulenko TN, Zhang P. Fibroblast growth factor and vascular endothelial growth factor play a critical role in endotheliogenesis from human adipose-derived stem cells. J Vasc Surg. 2017;65(5):1483–1492.

8. Bobyleva PI, Andreeva ER, Gornostaeva AN, Buravkova LB. Tissue-related hypoxia attenuates proinflammatory effects of allogeneic pbmcs on adipose-derived stromal cells in vitro. Stem Cells Int. 2016;2016:4726267.

9. Hattori H, Ishihara M. Altered protein secretions during interactions between adipose tissue- or bone marrow-derived stromal cells and inflammatory cells. Stem Cell Res Ther. 2015;6:70.

10. Kono TM, Sims EK, Moss DR, Yamamoto W, Ahn G, Diamond J, Tong X, Day KH, Territo PR, Hanenberg H, Traktuev DO, March KL, Evans-Molina C. Human adipose-derived stromal/stem cells protect against STZ-induced hyperglycemia: analysis of hASC-derived paracrine effectors. Stem Cells. 2014;32(7):1831–1842.

11. Eto H, Kato H, Suga H, Aoi N, Doi K, Kuno S, Yoshimura K. The fate of adipocytes after nonvascularized fat grafting: evidence of early death and replacement of adipocytes. Plast Reconstr Surg. 2012;129(5):1081–1092.

12. Tang Q, Chen C, Wang X, Li W, Zhang Y, Wang M, Jing W, Wang H, Guo W, Tian W. Botulinum toxin A improves adipose tissue engraftment by promoting cell proliferation, adipogenesis and angiogenesis. Int J Mol Med. 2017;40(3):713–720.

13. Li F, Guo W, Li K, Yu M, Tang W, Wang H, Tian W. Improved fat graft survival by different volume fractions of platelet-rich plasma and adipose-derived stem cells. Aesthet Surg J. 2015;35(3):319–333.

14. Shen J, Zhao Z, Shang W, Liu C, Zhang B, Zhao L, Cai H. Ginsenoside Rg1 nanoparticle penetrating the blood-brain barrier to improve the cerebral function of diabetic rats complicated with cerebral infarction. Int J Nanomedicine. 2017;12:6477–6486.

15. Tang B, Wang D, Li M, Wu Q, Yang Q, Shi W, Chen C. An in vivo study of hypoxia-inducible factor-1α signaling in ginsenoside Rg1-mediated brain repair after hypoxia/ischemia brain injury. Pediatr Res. 2017;81(1 -1):120–126.

16. Deng Y, Zhang T, Teng F, Li D, Xu F, Cho K, Xu J, Yin J, Zhang L, Liu Q, Yang M, Wu W, Liu X, Guo DA, Jiang B. Ginsenoside Rg1 and Rb1, in combination with salvianolic acid B, play different roles in myocardial infarction in rats. Chin Med Assoc. 2015;78(2):114–120.

17. Jiang M, Kang L, Wang Y, Zhao X, Liu X, Xu L, Li Z. A metabonomic study of cardioprotection of ginsenosides, schizandrin, and ophiopogonin D against acute myocardial infarction in rats. BMC Complement Altern Med. 2014;14:350.

18. Kwok HH, Chan LS, Poon PY, Yue PY, Wong RN. Ginsenoside-Rg1 induces angiogenesis by the inverse regulation of MET tyrosine kinase receptor expression through miR-23a. Toxicol Appl Pharmacol. 2015;287(3):276–283.

19. Chan LS, Yue PY, Wong YY, Wong RN. MicroRNA-15b contributes to ginsenoside-Rg1-induced angiogenesis through increased expression of VEGFR-2. Biochem Pharmacol. 2013;86(3):392–400.

20. Yang N, Chen P, Tao Z, Zhou N, Gong X, Xu Z, Zhang M, Zhang D, Chen B, Tao Z, Yang Z. Beneficial effects of ginsenoside-Rg1 on ischemia-induced angiogenesis in diabetic mice. Acta Biochim Biophys Sin (Shanghai). 2012;44(12):999–1005.

21. Shi AW, Gu N, Liu XM, Wang X, Peng YZ. Ginsenoside Rg1 enhances endothelial progenitor cell angiogenic potency and prevents senescence in vitro. J Int Med Res. 2011;39(4):1306–1318.

22. Xu FT, Li HM, Yin QS, Cui SE, Liu DL, Nan H, Han ZA, Xu KM. Effect of ginsenoside Rg1 on proliferation and neural phenotype differentiation of human adipose-derived stem cells in vitro. Can J Physiol Pharmacol. 2014;92(6):467–475.

23. Dong J, Zhu G, Wang TC, Shi FS. Ginsenoside Rg1 promotes neural differentiation of mouse adipose-derived stem cells via

the miRNA-124 signaling pathway. J Zhejiang Univ Sci B. 2017;18(5):445–448.

24. Xu FT, Liang ZJ, Li HM, Peng QL, Huang MH, Li de Q, Liang YD, Chi GY, Li de H, Yu BC, Huang JR. Ginsenoside Rg1 and platelet-rich fibrin enhance human breast adipose-derived stem cell function for soft tissue regeneration. Oncotarget. 2016; 7(23):35390–35403.

25. Xu FT, Li HM, Zhao CY, Liang ZJ, Huang MH, Li Q, Chen YC, Chi GY. Characterization of chondrogenic gene expression and cartilage phenotype differentiation in human breast adipose-derived stem cells promoted by ginsenoside Rg1 in vitro. Cell Physiol Biochem. 2015;37(5):1890–1902.

26. Luan A, Duscher D, Whittam AJ, Paik KJ, Zielins ER, Brett EA, Atashroo DA, Hu MS, Lee GK, Gurtner GC, Longaker MT, Wan DC. Cell-Assisted Lipotransfer Improves Volume Retention in Irradiated Recipient Sites and Rescues Radiation-Induced Skin Changes. Stem Cells. 2016;4(3): 668–673.

27. Han YD, Bai Y, Yan XL, Ren J, Zeng Q, Li XD, Pei XT, Han Y. Co-transplantation of exosomes derived from hypoxia-preconditioned adipose mesenchymal stem cells promotes neovascularization and graft survival in fat grafting. Biochem Biophys Res Commun. 2018;497(1):305–312.

28. Zhang J, Bai X, Zhao B, Wang Y, Su L, Chang P, Wang X, Han S, Gao J, Hu X, Hu D, Liu X. Allogeneic adipose-derived stem cells promote survival of fat grafts in immunocompetent diabetic rats. Cell Tissue Res. 2016;364(2):357–367.

29. Kølle SF, Fischer-Nielsen A, Mathiasen AB, Elberg JJ, Oliveri RS, Glovinski PV, Kastrup J, Kirchhoff M, Rasmussen BS, Talman ML, Thomsen C, Dickmeiss E, Drzewiecki KT. Enrichment of autologous fat grafts with ex-vivo expanded adipose tissue-derived stem cells for graft survival: A randomised placebo controlled trial. Lancet. 2013;382:1113–1120.

30. Saler M, Caliogna L, Botta L, Benazzo F, Riva F, Gastaldi G. hASC and DFAT, multipotent stem cells for regenerative medicine: a comparison of their potential differentiation in vitro. Int J Mol Sci. 2017;18(12). pii: E2699.

31. Jun-Jiang C, Huan-Jiu X. Vascular endothelial growth factor 165-transfected adipose-derived mesenchymal stem cells promote vascularization-assisted fat transplantation. Artif Cells Nanomed Biotechnol. 2016;44(4):1141–1149.

32. Jung DW, Kim YH, Kim TG, Lee JH, Chung KJ, Lim JO, Choi JY. Improvement of fat transplantation: fat graft with adipose-derived stem cells and oxygen-generating microspheres. Ann Plast Surg. 2015;5(4):463–470.

33. Yuan Y, Gao J, Lu F. Effect of exogenous adipose-derived stem cells in the early stages following free fat transplantation. Exp Ther Med. 2015;10(3):1052–1058.

34. Xu FT, Li HM, Yin QS, Liu DL, Nan H, Zhao PR, Liang SW. Human breast adipose-derived stem cells transfected with the stromal cell-derived factor-1 receptor CXCR4 exhibit enhanced viability in human autologous free fat grafts. Cell Physiol Biochem. 2014;34(6):2091–2104.

35. Xie Q, Xie J, Zhong J, Cun X, Lin S, Lin Y, Cai X. Hypoxia enhances angiogenesis in an adipose-derived stromal cell/endothelial cell co-culture 3D gel model. Cell Prolif. 2016; 49(2):236–245.

36. Wang J, Hao H, Huang H, Chen D, Han Y, Han W. The effect of adipose-derived stem cells on full-thickness skin grafts. Biomed Res Int. 2016;2016:1464725.

37. De Francesco F, Guastafierro A, Nicoletti G, Razzano S, Riccio M, Ferraro GA. The selective centrifugation ensures a better in vitro isolation of ASCs and restores a soft tissue regeneration in vivo. Int J Mol Sci. 2017;18(5). pii: E1038.

38. Tan SS, Zhan W, Poon CJ, Han X, Marre D, Boodhun S, Palmer JA, Mitchell GM, Morrison WA. Melatonin promotes survival of nonvascularized fat grafts and enhances the viability and migration of human adipose-derived stem cells via down-regulation of acute inflammatory cytokines. J Tissue Eng Regen Med. 2018;12(2):382–392.

39. Chen X, Yan L, Guo Z, Chen Z, Chen Y, Li M, Huang C, Zhang X, Chen L. Adipose-derived mesenchymal stem cells promote the survival of fat grafts via crosstalk between the Nrf2 and TLR4 pathways. Cell Death Dis. 2016;7(9): e2369.

40. Rasmussen BS, Lykke Sørensen C, Vester-Glowinski PV, Herly M, Trojahn Kølle SF, Fischer-Nielsen A, Drzewiecki KT. Effect, feasibility, and clinical relevance of cell enrichment in large volume fat grafting: a systematic review. Aesthet Surg J. 2017;7(Suppl 3): S46–S58.